Genetic and physiological responses to light quality in a deep ocean ecotype of *Ostreococcus*, an ecologically important photosynthetic picoeukaryote

[1,2]Elizabeth Sands, [1,3]Sian Davies, [1]Richard John Puxty, [4]Valerie Vergé, [4]François-Yves Bouget, [1]David John Scanlan and [1]Isabelle Alice Carré*

[1]School of Life Sciences, University of Warwick, Coventry, CV4 7AL, UK

[2]Department of Ecology and Environmental Sciences, Faculty of Science and Technology, Umeå University, 901 87 Umeå, Sweden

[3]Micropathology Ltd, Venture Centre, University of Warwick Science Park, Sir William Lyons Road, Coventry, CV4 7EZ, UK

[4]Université Pierre et Marie Curie, Paris 06, UMR 7621, Laboratoire d'Océanographie Microbienne, Observatoire Océanologique, Banyuls sur Mer, France

*Corresponding author: isabelle.carre@warwick.ac.uk

ORCIDs

Elizabeth Sands: 0000-0002-9569-2630

Sian Davies: 0000-0001-9892-6853

Richard John Puxty: 0000-0001-5564-2586

Valerie Vergé: 0000-0002-4149-8082

François-Yves Bouget: 0000-0001-7652-4490

David John Scanlan: 0000-0003-3093-4245

Isabelle Carré: 0000-0002-0548-7378

Highlight

We characterise the effects of light quality on the transcriptome and photophysiology of *Ostreococcus*, a photosynthetic picoeukaryote. We show that responses are distinct between two ecotypes originating from different environments, and that differences are linked to the gain or loss of transcription factor binding sites in the promoters of light-quality responsive genes.

Abstract

Phytoplankton are exposed to dramatic variations in light quality when cells are carried by upwelling or downwelling currents or encounter sediment. We investigated the potential impact of light quality changes in *Ostreococcus,* a key marine photosynthetic picoeukaryote, by analysing changes in its transcriptome, pigment content and photophysiology after acclimation to monochromatic red, green or blue light. The clade B species RCC809, isolated from the deep euphotic zone of the tropical Atlantic Ocean, responded to blue light by accelerating cell division at the expense of storage reserves and by increasing the relative level of blue-light absorbing pigments. RCC809 responded to red and green light by increasing its potential for photoprotection. In contrast, the clade A species OTTH0595, which originates from a shallow water environment, showed no difference in photosynthetic properties and minor differences in carotenoid contents between light qualities. This was associated with the loss of candidate lightquality responsive promoter motifs identified in RCC809 genes. These results demonstrate that light quality can have a major influence on the physiology of eukaryotic phytoplankton and suggest that different light quality environments can drive selection for diverse patterns of responsiveness and environmental niche partitioning.

Key words:

Light quality, phytoplankton, *Ostreococcus*, picoeukaryote, niche partitioning, transcriptomic analysis, photophysiology

Introduction

Phytoplankton are a vital part of the marine ecosystem. As primary producers, they provide a source of energy for the food web. They cycle nutrients, form a sink for carbon, and are responsible for roughly half the oxygen released to the atmosphere globally (Kulk *et al.*, 2020). Photosynthetic picoeukaryotes make a major contribution to these processes, being responsible for 25-44 % of global carbon capture (Jardillier *et al.*, 2010; Kirkham *et al.*, 2013; Mullin, 2001; Rii *et al.*, 2016). It is therefore important to understand how these organisms adapt to various ecological niches in the ocean, and to identify the environmental factors that influence their abundance. Here, we investigate the effects of light quality, a factor which is generally under-recognised in the marine environment.

Whilst the spectrum of incident light must match the absorption spectrum of photopigments for efficient photosynthesis, light quality can also serve as an indicator of competition by other organisms and initiate changes in growth strategy. On land, the light environment is broadly composed of light across the visible spectrum. Land plants possess blue, red, far-red and UV photoreceptors which enable them to respond to the spectral light environment. While red and blue light both promote photomorphogenesis, a low red to far-red ratio signifies shading by other plants. This triggers the shade avoidance response, which includes elongation of stems and petioles, an increase in leaf area, as well as accelerated flowering (Franklin and Whitelam, 2005). However, distinct factors influence light quality in oceanic systems (Bouman *et al.*, 2000). While visible light in the PAR range reaches a maximum depth of around 200 m, red, far-red and green light wavelengths are absorbed in the upper layers of the water column, so that only blue light reaches the deep euphotic zone. The light spectrum is also affected by the presence of particulates in coastal waters. Light absorption and scattering by dissolved organic matter and run-off from rivers causes a relative increase in yellow wavelengths (Erga *et al.*, 2012), while abundant phytoplankton increases the proportion of green light (Kume *et al.*, 2018; Lichtenthaler, 1987; Schubert *et al.*, 2001; Sun *et al.*, 2010; Tilzer *et al.*, 1995). Some species of cyanobacteria respond to these changes in light quality through a process known as complementary chromatic adaptation, in which levels of different phycobiliprotein pigments associated with the phycobilisome are adjusted to optimise absorption of excitation energy present in the environment (Sanfilippo *et al.*, 2019). However, much less is known about how eukaryotic microalgae respond to changes in light quality in their environment.

There is mounting evidence that a wide range of species of phytoplankton manifest a response, however. Light quality-dependent changes in photopigments were observed in diatoms, suggesting a form of chromatic adaptation (Brunet *et al.*, 2014; Hintz *et al.*, 2021; Xu *et al.*, 2021). Light quality was also found to affect the protein content of the red alga *Porphyra leucosticte* (Korbee *et al.*, 2005), the diatom *Cyclotella nana* and the green alga

Dunaliella tertiolecta (Wallen and Geen, 1971). It influenced the accumulation of lipids in the chlorophyte *Chlorella sp*. and in the heterokonts *Nannochloropsis oculata and Nannochloropsis gaditana* (Patelou *et al.*, 2020; Yuan *et al.*, 2020), as well as the growth rates of various phytoplankton species. Most species tested grew the fastest under blue light and the slowest under green light (Neun *et al.*, 2022; Patelou *et al.*, 2020; Yuan *et al.*, 2020), and blue light promoted the highest rate of growth in controlled mesocosm experiments with natural phytoplankton communities (Hintz *et al.*, 2021; Xu *et al.*, 2021). However, *Dunaliella salina* showed the fastest growth rates under red light (Li *et al.*, 2020) suggesting that diverging light quality responses may enable different species or ecotypes of microalgae to thrive in distinct environments, and to occupy different ecological niches.

Here, we investigated the effects of light quality on the transcriptome, pigment content and photophysiology *of Ostreococcus,* a photosynthetic picoeukaryote found in oceans across the world, including tropical and temperate environments (Limardo *et al.*, 2017; Rii *et al.*, 2016). We show that two ecotypes originating from distinct light quality environments exhibit contrasting responses. These findings suggest that the differential ability to respond to light quality signals may contribute to the specialisation of specific phytoplankton ecotypes to different environments.

Materials and Methods

Cell lines and growth conditions: *Ostreococcus* ecotypes RCC809 (a clone of RCC141) and OTTH0595 (also known as RCC745, RCC4221, OTTH0595 or *O. tauri*) were obtained from the Roscoff Culture Collection (http://roscoff-culture-collection.org). Cells were grown in Keller medium (Keller *et al.*, 1987). Batch cultures were incubated at 21 ^{o}C under diurnal light-dark cycles composed of 12 h light and 12 h darkness (12L12D) from cool-white fluorescent bulbs at an intensity of 20 μmol photons m^{-2} s^{-1}. They were transferred to fresh medium every 14 days.

Monochromatic light sources: Red and blue light was provided by LED arrays, and green light was provided by cool-white, fluorescent bulbs covered with one layer of green filter (Lee filter 139). Light intensity was the same under all conditions, i.e. 4 μmol photons m^{-2} s^{-1}. Emission spectra from these different light sources are shown in Fig. S1.

Determination of growth rates: Growth was monitored by measuring absorbance at 550 nm. Cell abundance was estimated based on the equation shown in Fig. S2. This relationship was the same for both the OTTH0595 and the RCC809 ecotypes under the different light conditions.

Determination of cell size: Flow cytometry measurements of forward scatter signal height (FSC-H) were carried out as described previously (Chretiennot-Dinet *et al.*, 1995; Mullaney *et al.*, 1969), 72 h after transfer to monochromatic light**.** Fluoresbrite Multifluorescent beads with an average diameter of 0.5 μm were used for calibration, in order to allow comparison of relative cell sizes between light conditions.

RNA-Seq experiment: Cells were grown in 200 ml cultures in 1 l flasks under white light as above until they reached mid to late log phase (20-40 million cells per ml). They were then transferred to constant monochromatic red, green, or blue light. After 72 h, cells were centrifuged at 5000 x *g*, pooled into 1 ml cold PBS, then spun again at maximum speed in a microfuge. The supernatant was discarded, and the cell pellet frozen in liquid nitrogen. For RNA extraction, 1 ml of TRIzol reagent was added to the frozen samples before thawing at room temperature. Two glass beads were added before shaking for 3 min using a Tissue Lyser (QIAGEN) at maximum speed. 200 μl of chloroform was added and mixed by shaking for 15 s before incubation at room temperature for 3 minutes and centrifugation at 12000 *g* at 4^{o}C for 15 minutes. The aqueous phase was transferred to a fresh tube, combined with 0.5 ml isopropanol and 5 μl of glycogen (20 mg/ml), incubated for 10 mins at room temperature, then spun down at 12000 x *g* at 4 ^{o}C for 15 mins. The supernatant was removed, and the pellet washed twice with 1 ml 70 % (v/v) ethanol before resuspension in 50 μl of RNase free water. Samples were treated with RNase-free DNase (Sigma-Aldrich) according to the manufacturer's instructions, before RNA purification using the Spectrum Plant Total RNA Kit (Sigma-Aldrich). RNA quality was verified using a Bioanalyser before preparation of RNA-Seq libraries using the Illumina Tru-Seq RNA library preparation kit, which enriches for mRNAs using Oligo-dT beads to capture polyA tails before cDNA synthesis. This method does not capture chloroplast RNA. 100 bp paired-end sequencing was carried out on an Illumina HiSeq at the Wellcome Trust.

RNA-Seq data were analysed within the Cyverse Discovery Environment (https://www.cyverse.org). Contaminating adapter sequences and poor quality sequences were removed using Trimmomatic v 0.36.0 (Bolger *et al.*, 2014). The Fastqc tool version 0.2 was then used to produce fastq files (Andrews, 2015), and TopHat version 2 to map reads to reference genomes using Bowtie 2 (Kim *et al.*, 2013; Langmead and Salzberg, 2012). Samples which gave low numbers of reads were removed from further analyses. CuffDiff version 2.2.1a was used to calculate differential expression values for each gene in each pair of samples (Trapnell *et al.*, 2013). Read counts were normalised by transcript length and by the total number of fragments, using the geometric Fragments per Kilobase of

Transcript per Million fragments mapped (FPKM) method. Differentially expressed genes were identified based on corrected p-values (q-values) and a false discovery rate (FDR) less than 0.05. This gave pairwise comparisons in the form of expression levels sorted by log2 fold change between each pair of light conditions. Gene expression patterns were visualised using the CummeRbund package (Goff *et al.*, 2014) and heatmaps were refined using the Pheatmap package (Kolde, 2019). Reference genomes used were the ORCAE OTTH0595 v2 genome (Blanc-Mathieu *et al.*, 2014; Derelle *et al.*, 2006; Palenik *et al.*, 2007) and the RCC809 v2 genome (Grigoriev *et al.*, 2012). Reference genome sequence (fasta) files and annotation (gff3) files for each *Ostreococcus* ecotype were sourced from the Online Resource for Community Annotation of Eukaryotes (ORCAE) database (http://bioinformatics.psb.ugent.be/orcae/).

Gene Ontology (GO) enrichment analyses and KEGG pathway mapping: OTTH0595 genes were annotated by compiling existing gene descriptions and GO terms from ORCAE and the Universal Protein knowledgebase (UniProt). In order to obtain GO term annotations for RCC809 genes, a genome-wide BLAST search of the NCBI non-redundant database was carried out using the Diamond BLASTx command line tool: 'translated Query-Protein Subject BLAST 2.2.31+' (E value 1.00E-03) (Camacho *et al.*, 2009). GO terms were then obtained using BLAST2GO software (Götz *et al.*, 2008). These annotations were compared to and merged with those available from the ORCAE and Interpro databases and with annotations from OTTH0595 homologues, identified by reciprocal BLAST. These were found to be consistent and, in some instances, more detailed than the existing annotations for RCC809. GO term over-representation analyses were carried out using the BiNGO 3.0.3 app in Cytoscape (Maere *et al.*, 2005). Multiple testing correction was carried out using Benjamini & Hochberg False Discovery Rate (FDR) correction with a significance cut-off at 0.05.

Pathway mapping using KEGG was carried out by searching for the homologues of the RCC809 enzymes in OTTH0595 as RCC809 is not yet listed on KEGG. These homologues were identified using a reciprocal genome-wide BLAST based on a minimum of 50 % identity.

Promoter motif identification: Analysis of the intergenic region length distribution in RCC809 showed a peak around 200 bp. This informed the selection of 250 bp regions upstream of start codons for promoter analyses. Coordinates of these regions were collected in bed files, listing the genomic coordinates for these promoter sequences. Fasta sequence files were then generated from the bed files using the GetFastaBed tool in Galaxy

(usegalaxy.org) (Gruening, 2014; Quinlan and Hall, 2010; The_Galaxy_Community, 2022). Short motifs that were over-represented in the promoters of light-responsive genes compared to a background of promoters genome-wide were identified using the Dreme 5.0.4 tool in the Meme suite (http://meme-suite.org) (Bailey, 2011). Matches to known or predicted binding sites for RCC809 transcription factors (TFs) were identified from the CIS-BP database using Motif Scan (Weirauch *et al.*, 2014).

Analysis of photosynthetic parameters: Cell cultures were grown under white light then acclimated to monochromatic light for 72 h before analysis of photosynthesis parameters using a PhytoPAM fluorometer. Cultures were diluted 5-fold before analysis to avoid saturation of the fluorescence signal. In order to determine the maximum quantum yield of photosystem II (PSII) photochemistry (F_v/F_m), samples were kept in darkness in the cuvette for 5 mins, so that the primary electron acceptor would be fully oxidised and a basal fluorescence level (F_0) could be measured. A saturating light pulse (2600 µmol photons m^{-2} s^{-1} at 470 nm) was then applied at 500 ms intervals and maximum fluorescence (F_m) was measured. To determine the effective quantum yield of PSII photochemistry (Φ_{PSII}), samples were subjected to increasing light intensities at 0, 3, 6, 36, 94, 124, 184, 213, 270, and 298 µmol photons $m^{-2}s^{-1}$ at 120 s intervals so that a fluorescence steady state Ft would be reached. Φ_{PSII} was calculated as (F_m'-F_t/F_m') using the Phyto-Win software (V 2.13). The Phyto-Win software also calculated the relative electron transport rate (rETR) as Yield x PAR x 0.5 x 0.84 µmol electrons $m^{-2}s^{-1}$, and used the Platt curve fitting model to provide alpha values and IK values from rapid light curve data (Platt *et al.*, 1980). The quantum yield of unregulated non-photochemical energy loss in PSII (ΦNO) was calculated as ΦNO = F/Fm, and the quantum yield of regulated non-photochemical energy loss (ΦNPQ) as ΦNPQ = (F/Fm')-(F/Fm) (Klughammer and Schreiber, 2008).

Pigment analyses

Cell cultures were grown under white light, then acclimated to monochromatic light for 72 hours as for the RNA-Seq experiment. Cell cultures were then harvested onto GF/F Glass Microfiber filters (Whatman) using a vacuum pump. The filters were immediately flash frozen in cryovials in liquid nitrogen and stored at -80 ^{o}C until shipped to the Danish Hydraulic Institute (DHI) laboratory in Denmark for analysis by high performance liquid chromatography (HPLC) as previously described (Van Heukelem and Thomas, 2001). Pigment standards were not available for uriolide, micromonal and dihydrolutein or for a previously described unknown carotenoid (Guyon *et al.*, 2018), so these were determined

using the response factor for β-carotene. The abundance of two chlorophyll *b*-like pigments in RCC809 was calculated using the chlorophyll *b* response factor.

Results

Blue light accelerates cell division in the RCC809 ecotype

The RCC809 ecotype of *Ostreococcus* was isolated from the deep euphotic zone of the tropical Atlantic. It is exposed to a range of light conditions in its natural enviornment, ranging from bright, broad spectrum light near the surface, to dim blue light near the bottom of the euphotic zone. While its responses to light intensity have been described previously (Six *et al.*, 2008; Six *et al.*, 2009), the effects of light quality have not been investigated.

To test the ability of RCC809 to grow under different qualities of monochromatic light, cultures were grown under white light until cell densities reached about 4 x 10^6 cells ml^{-1}, then transferred to red, green, or blue light of equivalent photosynthetically active radiation (PAR) of 4 μmol photons m^{-2} s^{-1}. RCC809 cultures grew faster under blue light, reaching cell densities almost twice higher than under red and green light by the end of the experiment (Fig. 1A).

To test whether the increased biomass under blue light might reflect changes in cell size rather than cell number, flow cytometry measurements of forward scatter signal height (FSC-H) were carried out. FSC-H was previously shown to positively correlate with cell size and was used to assess differences between *Ostreococcus* lineages (Mullaney *et al.*, 1969; Schaum *et al.*, 2016). However, no differences were observed between the different light conditions 72 h after transfer to red, blue or green light (Fig. 1B), indicating that differences in biomass were solely linked to different rates of cell division.

Transcriptional responses to light quality in RCC809

To gain insight into which biological processes were affected by light quality, we compared the transcriptomes of cultures that were acclimated to constant monochromatic red, green or blue light for 72 h (Fig. 2A). Differences in gene expression were analysed by RNA-Seq. Genes that were differentially expressed in pairwise comparisons between light qualities were identified based on corrected p-values and false discovery rates (FDR) less than 0.05 (Table 1, Supplementary dataset 1). Principal component analysis (PCA) showed that samples collected under different light qualities clustered into different groups, consistent with differential gene expression (Fig. 2B). Blue light samples were the most distinct, whereas red and green samples were more similar to each other. Thus, the majority of

differentially expressed genes had similar expression levels between red and green light conditions, but clearly different expression levels under blue light (Fig. 2C).

To separate gene expression responses by light quality, we identified genes whose expression was significantly increased or decreased under a given wavelength of light, compared to both others (Table 1). For example, genes that were induced by blue light were identified as significantly upregulated in blue light samples relative to both red and green light samples. This identified 536 genes that were specifically induced by blue light, and 472 that were repressed. Only 32 genes were induced and 14 repressed by red light, whereas 60 were induced and 159 repressed by green light (Table 1, Fig. 2D).

Motif over-representation analyses were then carried out to identify candidate regulatory elements responsible for the different types of responses. Potential matches to transcription binding sites were identified from the cis-BP database (Table 2). Remarkably, the most frequent motifs within the promoter sequences of light quality-responsive genes matched binding sites for MYB transcription factors. The sequence GATATTT, found to be over-represented within genes that were downregulated under red light, matched the known binding site for the MYB transcription factor CCA1 (Od04g00700), a light-responsive component of the *Ostreococcus* circadian clock (Corellou *et al.*, 2009). The motif GGATAG, predicted to be bound by the MYB protein Od06g01160, was over-represented within genes that were induced by red light, as well as within genes that were repressed by blue light. On the other hand, the motif CGATTC, predicted to be recognised by the MYB transcription factor Od12g02060, was over-represented within genes that were upregulated under blue light. The binding site for the cell-cycle related transcription factor E2F (GTTCCCC) was also over-represented in this group, consistent with the increased rate of cell division observed under blue light. The data further suggested potential roles for the sequence CCACGTGG and for a BHLH transcription factor (Od20g02280) to downregulate gene expression in response to blue light.

Effects of light quality on biological processes in RCC809

Gene ontology (GO) term analyses were carried out to test for enrichment of specific functional categories amongst light quality-responsive genes, relative to the rest of the genome. Differentially expressed genes were also mapped onto KEGG pathways to reveal potential metabolic consequences. This revealed effects of light quality on pathways related to cell division, primary metabolism, pigment biosynthesis and photosynthesis (Table 3).

41 genes related to the cell division cycle were differentially expressed under the different light qualities, including genes related to DNA replication, DNA repair and chromosome segregation (Table S1). Of these, 27 were upregulated under blue light relative to red and green light (Table S1). For example, the expression of cyclin-dependent kinase B

(Od14g01080), which is upregulated during S-phase in *Ostreococcus* (Corellou *et al.*, 2005; Farinas *et al.*, 2006), more than doubled under blue light (Fig. S3), and expression of two homologues (Od08g01730 and Od06g06460) of the Rad51 recombinase, which plays a role in double strand repair during DNA replication (Lim *et al.*, 2020), was upregulated in a similar manner. These observations were consistent with the faster growth rates observed in blue light relative to red and green light and suggested that exposure to blue light signals acceleration of the cell cycle in the RCC809 ecotype of *Ostreococcus*.

The RNA-Seq analysis also revealed changes in expression of genes with key roles in photosynthetic carbon fixation. Three different genes encoding the small subunit of RuBisCO (Od17g01990, Od17g02000 and Od17g02010) showed a 2-fold reduction in expression under blue light relative to red light, with intermediate levels being observed under green light (Fig. S4A-C). RuBisCO activase (Od04g02820), which enhances RuBisCO activity through removal of competitive inhibitors (Portis, 2003), showed similar trends (Fig. S4D) suggesting that exposure to blue light may lead to less efficient carbon fixation.

In addition, multiple enzymes in the glycolysis and gluconeogenesis pathways were downregulated under blue light (Fig. S5). While most of these enzymes had both catabolic and anabolic functions, the downregulation of four different fructose-1,6-bisphosphatase genes (Od09g06250, Od06g06980, Od03g02850 and Od20g01100) under blue light suggested a decrease in gluconeogenesis in this condition, while upregulation of pyruvate dehydrogenase suggested an increased rate of glycolysis. Genes associated with fatty acid biosynthesis were also downregulated under blue light (Fig. S6), whereas multiple enzymes in the TCA cycle were upregulated under blue light. This included citrate synthase (Od05g01850), which catalyses the first step of the cycle, and three genes encoding malate dehydrogenase (Od03g03160, Od06g02230, Od08g00070), which regenerates oxaloacetate from malate (Fig. S7). Altogether, these results suggested an increased rate of catabolism and a reduction in energy storage under blue light.

The gene expression data further suggested that synthesis of photopigments (chlorophylls and carotenoids) was globally reduced under blue light, relative to red and green light. 7 genes encoding enzymes in the plastidic MEP/DOXP terpenoid backbone biosynthesis pathway showed reduced expression levels under blue light, while only one showed lower expression under green light (Fig. S8). Multiple enzymes with roles in synthesis of porphyrin precursors of chlorophylls were also downregulated under blue light (Fig. S9A), including the enzyme glutamate-1-semialdehyde aminotransferase (GSA-AM) HemL (Od19g01200), which catalyses the production of 5-amino levulinic acid (dALA) from glutamate-1-semialdehyde and is rate-limiting in *Arabidopsis* (Sinha *et al.*, 2022).

Expression of chlorophyll *a* (chl*a*) synthase (Od08g01040) was downregulated under blue light (Fig. S9B). As this enzyme catalyses the last step of chl*a* biosynthesis, this

suggested potential shifts in the ratio of chl*b* to chl*a*. Furthermore, the expression of violaxanthin de-epoxidase (Od11g00170), which catalyses the conversion of violaxanthin to zeaxanthin, was elevated under blue light, whereas zeaxanthin epoxidase (Od02g02570), which catalyses the reverse reaction, was elevated under red light (Fig. S10A,B). A member of the CYP97 carotene hydroxylase family (Od09g03950) showed reduced expression under blue light compared to red light (Fig. S10C). As this enzyme plays a role in the conversion of carotenes to lutein (Cui *et al.*, 2013), this suggested that the synthesis of lutein and its derivatives may decrease under blue light.

Changes related to photosystems were also observed. Two genes with roles in the synthesis of phylloquinone (Od07g04840 and Od20g02670) were downregulated under blue light. Phylloquinone acts as a cofactor in Photosystem I (PSI)-mediated electron transport between the primary electron acceptor and ferredoxin, and a decrease in phylloquinone was previously shown to be associated with a decrease in PSI activity (Gross *et al.*, 2006). Six genes predicted to encode PSII assembly proteins showed also elevated expression under blue light, suggesting an increase in PSII content, but expression of another PSII component was reduced, suggesting a possible change in composition (Table S2).

Ostreococcus possesses multiple photoreceptors, including a phototropin, a light-oxygen-voltage-histidine kinase (LOV-HK), three cryptochromes, and a histidine kinase rhodopsin (HKR) (Djouani-Tahri *et al.*, 2011; Heijde *et al.*, 2010; Luck *et al.*, 2019; Sullivan *et al.*, 2016). While genes involved in light perception were not found to be significantly over-represented within any group of light quality-responsive genes, both genes encoding LOV-HK (Od09g04310 and Od09g04300) showed reduced expression under blue light compared to red light (Fig. S10). The phototropin photoreceptor (Od15g00300) and the cryptochrome OdCPF1 (Od05g00310) showed a similar response. In contrast, expression of the Cry-DASH cryptochrome OdCPF2 (Od01g00210) was elevated in blue light, whereas expression of the histidine kinase rhodopsin (HKR) photoreceptor (Od15g00300) was not affected by light quality.

Changes in pigment content and photosynthetic parameters in RCC809

To uncover the functional consequences of these changes in gene expression, HPLC analyses of cell pigment contents were carried out. This revealed elevated levels of several carotenoids under blue light relative to red and green light, including neoxanthin, micromonal, dihydrolutein, uriolide and a previously described, unknown carotenoid (Guyon *et al.*, 2018). In contrast, prasinoxanthin, violaxanthin and zeaxanthin levels were reduced (Fig. 3A).

Carotenoids and their oxygenated xanthophyll derivatives play important roles within light-harvesting complexes, both as accessory light-harvesting pigments and to protect the photosynthetic apparatus from damage by excessive light. The conversion of violaxanthin (V) to antheraxanthin (A) and zeaxanthin (Z) through the de-epoxidation reactions of the xanthophyll cycle acts to protect photosystem II from light damage through quenching of excessive excitation energy and dissipation into heat, a process known as non-photochemical quenching (NPQ) (Goss and Latowski, 2020). The xanthophyll cycle can also play a role in detoxification of reactive oxygen species (ROS) which are generated under supersaturating light conditions. To assess the potential for xanthophyll cycle induction for photoprotection, the total xanthophyll to chl*a* ratio was calculated as Z+A+V/chl*a*, where Z, A and V correspond to relative levels of zeaxanthin, antheraxanthin and violaxanthin, respectively (Demmig-Adams, 1990). This ratio was smaller under blue light than in red or green light, indicating a reduction in the total xanthophyll pool size under blue light relative to red or green light. (Fig. 3B). However, no differences were noted in the depoxidation state (DPS), calculated as (Z + 0.5A)/(V + A + Z) (Munné-Bosch and Cela, 2006) (Fig. 3C).

As predicted by the gene expression data, blue light induced an increase in chl*b* levels relative to chl*a* (Fig. 3D, E)**.** However, the most remarkable response to blue light was an approximately 10-fold increase in two unknown pigments, which were annotated as chl*b*-like based on their spectral similarity to chl*b* (Fig. 3D**;** Fig. S12). The chlorophyll metabolite Mg-2,4-divinyl pheoporphyrin (MgDVP), which plays a role as a light harvesting accessory pigment, also increased significantly relative to chl*a*, almost doubling in blue light compared to both red and green light (Fig. 3D). Altogether these results demonstrated that light quality influences the pigment composition of the RCC809 strain of *Ostreococcus*, with potential consequences for light-harvesting efficiency.

To test the consequences of these pigment responses for photosynthetic activity, PAM (pulse-amplitude modulation) fluorometry analysis was used to compare the efficiency of photosystem II after acclimation to the different light qualities. We first assayed the quantum yield of PSII photochemistry (Φ_{PSII}) under short pulses of increasing light intensity at 470 nm (Ralph and Gademann, 2005). As expected, the quantum yield of PSII was highest in response to low intensity light pulses where carbon fixation operates at maximum photosynthetic efficiency, and decreased at higher light intensities as electron transfer pathways became saturated (Fig. 4A). While similar changes were observed in cells adapted to different light conditions, Φ_{PSII} was always highest in cells acclimated to red light and lowest in cells acclimated to blue light at a given intensity of excitatory light.

The relative electron transport rate (rETR) increased with the intensity of excitation, reaching a plateau around 50-150 μmol photons m^{-2} s^{-1}, then decreased at higher light

intensities (Fig. 4B). Higher electron transfer rates were observed in cells acclimated to red light, and lower rates in cells acclimated to blue light. Furthermore, saturation was reached at a lower intensity in cells acclimated to blue light than in cells acclimated to red light (about 30 and 50 μmol photons m^{-2} s^{-1}, respectively, as indicated by IK values in Figure 4E). These findings suggest that the photosynthetic machinery in RCC809 can utilise light energy more efficiently after acclimation to red light as compared to blue light. Cells acclimated to green light showed an intermediate phenotype.

Photoprotection processes were also impacted by light quality. Consistent with the increased total xanthophyll pool size under red light, ΦNPQ values were elevated under this light condition (Fig. 4C), indicating an increased capacity for photoprotection through processes regulated by the transthylakoid proton gradient (Kramer *et al.*, 2004). Conversely, ΦNO values, which quantify energy dissipation through unregulated processes were highest under blue light (Fig. 4D). This suggested that cells acclimated to this wavelength were less able to protect themselves against damage by excess illumination.

Φ_{PSII} and rETR values under green light were intermediate between those under red and blue light (Fig. 4A,B). However, ΦNPQ and ΦNO values under green light were similar to those under blue light (Fig. 4C,D), suggesting that green light did not induce photoprotection in spite of the increased xanthophyll pool size relative to blue light.

Light quality responses are attenuated in OTTH0595, a shallow water ecotype of *Ostreococcus*

While light intensity is thought to be the primary abiotic factor determining the clade distribution of *Ostreococcus* species (Botebol *et al.*, 2017; Demir-Hilton *et al.*, 2011; Rodriguez *et al.*, 2005; Six *et al.*, 2009), we hypothesised that light quality may also play a role. Our prediction was that an ecotype originating from a shallow water environment and exposed to the full visible light spectrum at all times, may exhibit distinct responses to light quality from a deep ocean ecotype, which is exposed to variable wavelengths of light as it is moved up and down the water column. We therefore compared the light quality responses of the deep ocean ecotype RCC809, with those of the lagoon species OTTH0595, also known as *O. tauri*.

OTTH0595 growth rates were similar under all light qualities and only slightly slower under red light compared to blue and green light (Fig. 5A). HPLC analyses revealed that the chl*b*:chl*a* ratio was not affected by light quality (Fig. 5B). Small increases in micromonal and dihydrolutein contents were observed in blue light (9% and 14 %, respectively; Fig. 5**c**), but these were minor changes compared to those observed in RCC809 (43% and 52%, respectively). Consistent with previous observations that OTTH0595 tolerates higher light

intensities (Cardol *et al.*, 2008; Demir-Hilton *et al.*, 2011; Six *et al.*, 2008; Six *et al.*, 2009), rETR values were higher than in RCC809 and did not decrease at high light intensities. However, no significant differences in PSII quantum yield or rETR were observed between light qualities (Fig. 5D,E).

To examine whether the attenuated light responses of the OTTH0595 species were linked to divergence in gene regulation relative to RCC809, we identified the OTTH0595 homologues of light quality-responsive genes from RCC809 and examined their upstream regulatory sequences for the presence or absence of the candidate regulatory elements identified in Table 2. While the GTTCCCC[T/C] motif, recognised by the cell cycle-related transcription factor E2F, was conserved in 80 % of OTTH0595 homologues, other motifs were only present in 30 to 40 % of OTTH0595 genes, suggesting that they either had been lost in OTTH0595 or gained in RCC809 during the course of their evolutionary divergence (Fig. 5F).

Discussion

Blue light signals a distinct growth strategy from red and green light in RCC809

Our results demonstrate that the *Ostreococcus* ecotype RCC809 exhibits responses to light quality. Transcriptomic analyses revealed differences in gene expression between cells acclimated to red, green, and blue monochromatic light. Gene expression under blue light was most distinct from red light, whilst intermediate phenotypes were seen under green light. *Ostreococcus* responses to light quality contrasted with those of land plants, where the effects of green light oppose those of red and blue wavelengths (Wang and Folta, 2013). This distinct pattern of light quality responses may be linked to the presence of a different set of photoreceptors. While cryptochrome and phototropin photoreceptors are present across all plants and algae (Kianianmomeni and Hallmann, 2014) , *Ostreococcus* contains the histidine kinases LOV-HK and HKR which are absent in land plants but does not contain phytochomes.

LOV-HK and HKR may be responsible for responses to blue and green light, respectively (Djouani-Tahri *et al.*, 2011) (Luck *et al.*, 2019), but the identity of the photoreceptor responsible for perception of red light remains unclear.

Blue light signalled a switch in physiology and metabolism to a state that favoured growth at the expense of energy storage (Fig. 6). Thus, acclimation to blue light resulted in the elevated expression of genes associated with the cell cycle and faster growth rates. Conversely, expression of enzymes involved in starch or fatty acid biosynthesis was reduced

in blue light, whereas the expression of TCA cycle enzymes was elevated. Exposure to green or red light elicited the opposite response.

We questioned whether the gene expression signatures observed under green light might represent a starvation response due to poor absorption of light by chlorophylls in this part of the spectrum. However, the fact that similar responses were observed under red and green light argued against this, because red light is absorbed efficiently by chlorophylls (Liu and van Iersel, 2021). Furthermore, the growth arrest observed under red or green light was accompanied by upregulation of starch and fatty acid biosynthesis pathways, which is not consistent with a starvation response. We suggest that enrichment of red or green wavelengths may signal conditions less favourable for growth in the natural environment, such as shading by sediments or other particulate material, competition from other organisms, or exposure to damaging light intensities near the surface.

RCC809 adjusts its pigment contents and photosystem function as a function of the light quality environment

Previous work showed that increases in light intensity induce the downregulation of both chl*a* and chl*b* content, accumulation of lutein, and increased xanthophyll de-epoxidation in the RCC809 ecotype of *Ostreococcus* (Six *et al.*, 2008). Blue light triggered a distinct set of responses in our experiment, suggesting that cells did not respond to the higher energy levels carried by blue wavelengths, but rather to the specific light quality.

Blue light induced an increase in the carotenoid pigments dihydrolutein and micromonal, as well as an increase in MgDVP, chl*b* and chl*b*-like pigments relative to chl*a*. This was consistent with chromatic adaptation, as chl*b* and MgDVP absorb much more under blue light than chl*a* and these changes would be expected to enhance cells' ability to utilise blue light for photosynthesis (Raven, 1996).

In contrast, red and green light induced expression of enzymes involved in the biosynthesis of chl*a*, which would be predicted to increase light absorption under red light. Whilst the lower chl*b*:chl*a* ratio suggested that the size of the photosynthetic antenna was smaller in cells acclimated to red light, PSII efficiency was increased as indicated by higher PSII quantum yield and rETR values. This may be linked to higher RuBisCO activity, as the expression of RuBisCO small subunits and of RuBisCO activase was higher under red and green light, compared to blue light, and the RuBisCo activation state is known to be positively correlated with the electron transport rate in higher plants (Perdomo *et al.*, 2017).

An increase in the total xanthophyll pool size was also observed under red and green light, indicating an increased potential for photoprotection. Consistent with this observation,

red or green light-adapted cultures maintained higher PSII quantum yields and rETR under increasing light intensities. However, increased ΦNPQ values were only observed following acclimation to red light, indicating that only red light induced photoprotection. This suggests that while both red and green light signal unfavourable growth conditions, perception of red light may specifically signal proximity to the surface and allow cells to anticipate exposure to high light intensities through induction of photoprotective mechanisms (Fig. 6).

Evidence for adaptation to different light quality environments

We compared the light quality responses of the RCC809 ecotype, isolated from the tropical Atlantic Ocean at a depth of 105 metres, with those of the lagoon ecotype OTTH0595. These two *Ostreococcus* species were previously shown to belong to distinct clades (Demir-Hilton *et al.*, 2011) and to exhibit distinct responses to light intensity (Cardol *et al.*, 2008; Six *et al.*, 2008; Six *et al.*, 2009). OTTH0595 originates from shallow environments where it is not greatly affected by the narrowing of spectral availability associated with depth (Potes *et al.*, 2013). Instead, the spectral quality varies mostly according to the level of suspended sediment and other photosynthetic organisms. It may therefore be less important for this species to be able to perceive the blue-light enriched environment associated with depth, and to adjust its photosystems accordingly. Furthermore, OTTH0595 showed no differences in pigment content when adapted to different light qualities, except for a small increase in dihydrolutein and micromonal under blue light, and its PSII quantum yield and rETR were unaffected.

While OTTH0595 possesses the same set of photoreceptors as RCC809, mechanistic clues to their distinct responses to light quality may be obtained through investigation of promoter motifs and their cognate transcription factors. Analysis of over-represented motifs within RCC809 light quality-responsive promoters identified a number of candidate regulatory motifs, including binding sites for MYB and bHLH transcription factors. Remarkably, most of these promoter motifs were missing from OTTH0595 homologues of RCC809 light quality- responsive genes, suggesting a lack of selective pressure for such regulation in OTTH0595. Furthermore, a single bHLH transcription factor was identified in OTTH0595, as compared to four in RCC809, suggesting the loss of light-responsive transcription factors. Our findings suggest that distinct light quality environments in the aquatic environments can result in different evolutionary pressures and may select for gain or loss of regulatory connections downstream of photoreceptors.

Perspectives

Taken together, these observations suggest that, whilst light intensity has been considered the primary abiotic factor determining the distribution of *Ostreococcus* ecotypes, differences in light quality responses of ecotypes should also be considered as an important factor in determining adaptation to distinct environmental niches. Further work will be required, however, to determine whether our observations can be generalised to other *Ostreococcus* species. These were previously classified into 4 different clades, based on small ribosomal RNA gene sequences (Guillou *et al.*, 2004; Subirana *et al.*, 2013). RCC809 and OTTH0595 (also known as *O. tauri*) belong to clades B and C. Clades A and D include *O. lucimarinus* and *O. mediterraneus*, respectively (Subirana *et al.*, 2013; Worden *et al.*, 2004), and are associated with relatively shallow coastal zones (Demir-Hilton *et al.*, 2011; Limardo *et al.*, 2017). While the distribution of these species was previously proposed to be driven by differences in temperature, salinity, nutrient abundance and light intensity, our findings suggest that light quality may also contribute. Based on the similarity of their light environment to OTTH95, clade B and C species are predicted to exhibit very limited responses to light quality.

It remains unclear how *Ostreococcus*' responses to light quality contribute to fitness in different environments. Future metatranscriptomic analyses may provide valuable clues by revealing where these responses are observed in nature. We hypothesise that what was described here as responses to red or green light may be observed near the surface, whereas blue light responses would be observed at depth. However, such analyses are likely to be complicated by varying light intensities, and the fact that cells in the natural environment are exposed to the full spectrum of light.

It also remains to be determined whether our findings in *Ostreococcus* RCC809 apply to other types of eukaryotic phytoplankton. While few detailed transcriptomic analyses are available, there is mounting evidence that other species of microalgae exhibit responses to light quality, affecting carbon metabolism and lipid accumulation (Lehmuskero *et al.*, 2018; Maltsev *et al.*, 2021), pigment composition (Maltsev *et al.*, 2021; Rochet *et al.*, 1986; Valle *et al.*, 2014; Wei *et al.*, 2020), and rates of cell division (Neun *et al.*, 2022). The specific responses vary between organisms, however. For example, the diatom *Phaeodactylum tricornutum* (CCMP2561) grew faster under blue light than under red light (Huysman *et al.*, 2013). This was associated with induction of the cell cycle protein *diatom-specific cyclin2* (*DSCYC2*) through activation of the diatom-specific photoreceptor aureochrome and of the cryptochrome/photolyase CPF1 (Coesel *et al.*, 2009; Huysman *et al.*, 2013). Blue light also promoted the growth of the green algae *Chlorella sp.* HQ (Liu *et al.*, 2021) and *Chlorella pyrenoidosa* (Guo and Fang, 2020). In contrast, yellow and red wavelengths were reported

to promote faster growth of *Chlorella vulgaris* and *Dunaliella salina* than blue light (Hultberg *et al.*, 2014; Li *et al.*, 2020),

Light quality was found to affect photoprotective responses in a broad range of microalgae. Blue light induced accumulation of chlorophyll and carotenoid pigments in *Chlorella Sp HQ* (Liu *et al.*, 2021), *Chlamydomonas reinhardtii* (Redekop *et al.*, 2022), *Nannochloropsis oceanica* (Wei *et al.*, 2020), *Dunalliella salina* (Li *et al.*, 2020) and *Phaeodactylum tricornutum strain IO 108–01* (Duarte *et al.*, 2021). Blue light induced expression of the photoprotective genes *LHCSR1*, *LHCSR3.1* and *PSBS1* in *Chlamydomonas reinhardtii* (Redekop *et al.*, 2022), and the induction of energy-dependent quenching (qE quenching) required phototropin, a blue light photoreceptor (Petroutsos et al., 2016; Aihara et al., 2019; Redekop *et al.*, 2022). Blue light also promoted expression of photoprotective, ROS-scavenging enzymes in *Dunaliella salina* (Li *et al.*, 2020). In contrast, ROS scavenging pathways were upregulated under red light in *Nannochloropsis oceanica* (Wei *et al.*, 2020). In *Phaeodactylum tricornutum*, different studies showed induction of photo protective responses by different light qualities, and these apparent discrepancies may in fact reflect differences between strains. Thus, blue light induced an increase in xanthophyll pool size in strain UTEX 646 (Schellenberger Costa *et al.*, 2012) and the expression of genes involved in repair of photodamaged PSI and ROS scavenging in strain CCMP632 (Valle *et al.*, 2014). However, red light induced accumulation of fucoxanthin in strain IO 108–01, resulting in a higher potential for photoprotection than under blue light (Duarte *et al.*, 2021). These observations, together with the results presented here, suggest that differences in light quality responses between eukaryotic microalgae can arise within relatively close taxonomic groups.

Our findings suggest that light quality in the aquatic environment represents a significant evolutionary pressure which can lead to extensive rewiring of transcriptional responses downstream of photoreceptors. The suppression of some responses and the acquisition of others through loss or gain of transcription factor binding sites in the promoters of light-responsive genes may allow different phytoplankton species to differentiate their light quality responses from each other, enabling the colonisation of distinct niches in the environment. The spectral tuning of photoreceptors and their loss in some algal lineages may also contribute to adaptation to different aquatic environments (Jaubert *et al.*, 2017). Changes in ocean colour resulting from climate change will lead to ecosystem changes (Cael *et al.*, 2023). It will be important to understand how light quality responses contribute to the fitness of different phytoplankton species, in order to predict the consequences of these changes for the global distribution of these primary producers in the oceans and for the aquatic food chain.

Acknowledgements: The RCC809 and OTTH0595 cell lines were obtained from the Roscoff culture collection. Sequencing of RNA-Seq samples was carried out at the Wellcome Trust, and RNA-Seq data were analysed within the Cyverse Discovery Environment (https://cyverse.org).

Conflict of interest: No conflict of interest declared.

Funding: The work was supported by a studentship from the Central England NERC Training Alliance (CENTA) to ES, and by funding from the European Union's Horizon 2020 research and innovation programme to ES and IAC, under grant agreement No 730984, ASSEMBLE Plus project.

Author contributions

SD prepared the samples used in RNA-Seq analyses. ES analysed the RNA-Seq data, performed growth, pigment and PhytoPAM analyses. RP assisted with PhytoPAM analyses. VV carried out growth experiments. DS and IAC conceived and supervised the project. FYB assisted with preliminary experiments. ES and IAC prepared the manuscript.

Data availability

The transcriptomics dataset was deposited in the Gene Expression Omnibus database under accession number GSE221420.

References

Aihara Y, Fujimura-Kamada K, Yamasaki T *et al.* . 2019. Algal photoprotection is regulated by the E3 ligase CUL4–DDB1^{DET1}. Nature Plants 5, 34–40.

Andrews S. 2015. FastQC: A quality control tool for high throughput sequence data. http://www.bioinformatics.babraham.ac.uk/projects/fastqc/

Bailey TL. 2011. DREME: motif discovery in transcription factor ChIP-seq data. Bioinformatics doi: 10.1093/bioinformatics/btr261

Blanc-Mathieu R, Verhelst B, Derelle E, *et al*. 2014. An improved genome of the model marine alga *Ostreococcus tauri* unfolds by assessing Illumina de novo assemblies. BioMed Central Genomics doi: 10.1186/1471-2164-15-1103

Bolger AM, Lohse M, Usadel B. 2014. Trimmomatic: a flexible trimmer for Illumina sequence data. Bioinformatics doi: 10.1093/bioinformatics/btu170

Botebol H, Lelandais G, Six C, *et al*. 2017. Acclimation of a low iron adapted *Ostreococcus* strain to iron limitation through cell biomass lowering. Scientific Reports doi: 10.1038/s41598-017-00216-6

Bouman HA, Platt T, Kraay GW, Sathyendranath S, Irwin BD. 2000. Bio-optical properties of the subtropical North Atlantic. I. Vertical variability. Marine Ecology Progress Series 200, 3-18.

Brunet C, Chandrasekaran R, Barra L, Giovagnetti V, Corato F, Ruban AV. 2014. Spectral Radiation Dependent Photoprotective Mechanism in the Diatom *Pseudo-nitzschia multistriata*. Plos One doi: 10.1371/journal.pone.0087015

Cael BB, Bisson K, Boss E, Dutkiewicz S, Henson S. 2023. Global climate-change trends detected in indicators of ocean ecology. Nature 619, 551-554.

Camacho C, Coulouris G, Avagyan V, Ma N, Papadopoulos J, Bealer K, Madden TL. 2009. BLAST+: architecture and applications. BioMed Central Bioinformatics doi: 10.1186/1471-2105-10-421

Cardol P, Bailleul B, Rappaport F, Derelle E, Beal D, Breyton C, Bailey S, Wollman F, Grossman A, Moreau H, Finazzi G. 2008. An original adaptation of photosynthesis in the marine green alga *Ostreococcus*. Proceedings of the National Academy of Sciences of the United States of America 105, 7881-7886.

Chretiennot-Dinet M, Courties C, Vaquer A, Neveux J, Claustre H, Lautier J, Machado M. 1995. A new marine picoeucaryote - *Ostreococcus tauri* gen et sp. nov (Chlorophyta, Prasinophyceae). Phycologia 34, 285-292.

Coesel S, Mangogna M, Ishikawa T, Heijde M, Rogato A, Finazzi G, Todo T, Bowler C, Falciatore A. 2009. Diatom PtCPF1 is a new cryptochrome/photolyase family member with DNA repair and transcription regulation activity. EMBO Reports 10, 655-661.

Corellou F, Camasses A, Ligat L, Peaucellier G, Bouget F. 2005. Atypical regulation of a green lineage-specific B-type cyclin-dependent kinase. Plant Physiology 138, 1627-1636.

Corellou F, Schwartz C, Motta J, Djouani-Tahri E, Sanchez F, Bouget F. 2009. Clocks in the green lineage: comparative functional analysis of the circadian architecture of the Picoeukaryote *Ostreococcus*. Plant Cell 21, 3436-3449.

Cui H, Yu X, Wang Y, Cui Y, Li X, Liu Z, Qin S. 2013. Evolutionary origins, molecular cloning and expression of carotenoid hydroxylases in eukaryotic photosynthetic algae. BioMed Central Genomics doi: 10.1186/1471-2164-14-457

Demir-Hilton E, Sudek S, Cuvelier ML, Gentemann CL, Zehr JP, Worden AZ. 2011. Global distribution patterns of distinct clades of the photosynthetic picoeukaryote *Ostreococcus*. The ISME Journal: Multidisciplinary Journal of Microbial Ecology 5, 1095-1107.

Demmig-Adams B. 1990. Carotenoids and photoprotection in plants: A role for the xanthophyll zeaxanthin. Biochimica et Biophysica Acta (BBA) - Bioenergetics 1020, 1-24.

Derelle E, Ferraz C, Rombauts S, et al. 2006. Genome analysis of the smallest free-living eukaryote *Ostreococcus tauri* unveils many unique features. Proceedings of the National Academy of Sciences of the United States of America 103, 11647-11652.

Djouani-Tahri E-B, Christie JM, Sanchez-Ferandin S, Sanchez F, Bouget F-Y, Corellou F. 2011. A eukaryotic LOV-histidine kinase with circadian clock function in the picoalga *Ostreococcus*. The Plant Journal 65, 578-588.

Duarte B, Feijão E, Goessling JW, Caçador I, Matos AR. 2021. Pigment and fatty Acid production under different light qualities in the diatom *Phaeodactylum tricornutum*. Applied Sciences doi: 10.3390/app11062550

Erga S, Ssebiyonga N, Frette O, Hamre B, Aure J, Strand O, Strohmeier T. 2012. Dynamics of phytoplankton distribution and photosynthetic capacity in a western Norwegian fjord during coastal upwelling: Effects on optical properties. Estuarine Coastal and Shelf Science 97, 91-103.

Farinas B, Mary C, de O Manes CL, Bhaud Y, Peaucellier G, Moreau H. 2006. Natural synchronisation for the study of cell division in the green unicellular alga *Ostreococcus tauri*. Plant Molecular Biology 60, 277-292.

Franklin KA, Whitelam GC. 2005. Phytochromes and Shade-avoidance Responses in Plants. Annals of Botany 96, 169-175.

Goff L, Trapnell C, Kelley D. 2014. Analysis, exploration, manipulation, and visualization of Cufflinks high-throughput sequencing data. http://compbio.mit.edu/cummeRbund/

Goss R, Latowski D. 2020. Lipid dependence of xanthophyll cycling in higher plants and Algae. Frontiers in Plant Science doi: 10.3389/fpls.2020.00455

Götz S, García-Gómez JM, Terol J, Williams TD, Nagaraj SH, Nueda MJ, Robles M, Talón M, Dopazo J, Conesa A. 2008. High-throughput functional annotation and data mining with the Blast2GO suite. Nucleic Acids Research 36, 3420-3435.

Grigoriev IV, Nordberg H, Shabalov I, *et al*. . 2012. The genome portal of the Department of Energy Joint Genome Institute. Nucleic Acids Research 40, D26-32.

Gross J, Cho WK, Lezhneva L, Falk J, Krupinska K, Shinozaki K, Seki M, Herrmann RG, Meurer J. 2006. A plant locus essential for phylloquinone (vitamin K1) biosynthesis

originated from a fusion of four eubacterial genes. Journal of Biological Chemistry 281, 17189-17196

Gruening BA. 2014. Galaxy Wrapper. https://github.com/bgruening/galaxytools

Guillou L, Eikrem W, Chrétiennot-Dinet M-J, Le Gall F, Massana R, Romari K, Pedrós-Alió C, Vaulot D. 2004. Diversity of Picoplanktonic Prasinophytes Assessed by Direct Nuclear SSU rDNA Sequencing of Environmental Samples and Novel Isolates Retrieved from Oceanic and Coastal Marine Ecosystems. Protist 155, 193-214.

Guo H, Fang Z. 2020. Effect of light quality on the cultivation of *Chlorella pyrenoidosa*. E3S Web Conf. doi: 10.1051/e3sconf/202014302033

Guyon JB, Vergé V, Schatt P, Lozano JC, Liennard M, Bouget FY. 2018. Comparative analysis of culture conditions for the optimization of carotenoid production in several strains of the picoeukaryote *Ostreococcus*. Marine Drugs doi: 10.3390/md16030076

Heijde M, Zabulon G, Corellou F, *et al*. .2010. Characterization of two members of the cryptochrome/photolyase family from *Ostreococcus tauri* provides insights into the origin and evolution of cryptochromes. Plant, Cell & Environment 33, 1614-1626.

Hintz NH, Zeising M, Striebel M. 2021. Changes in spectral quality of underwater light alter phytoplankton community composition. Limnology and Oceanography 66, 3327-3337.

Hultberg M, Jönsson HL, Bergstrand K-J, Carlsson AS. 2014. Impact of light quality on biomass production and fatty acid content in the microalga *Chlorella vulgaris*. Bioresource Technology 159, 465-467.

Huysman MJJ, Fortunato AE, Matthijs M, *et al*. .2013. AUREOCHROME1a-Mediated Induction of the Diatom-Specific Cyclin dsCYC2 Controls the Onset of Cell Division in Diatoms (*Phaeodactylum tricornutum*). Plant Cell 25, 215-228.

Jardillier L, Zubkov M, Pearman J, Scanlan D. 2010. Significant CO_2 fixation by small prymnesiophytes in the subtropical and tropical northeast Atlantic Ocean. The ISME Journal: Multidisciplinary Journal of Microbial Ecology 4, 1180-1192.

Jaubert M, Bouly J-P, Ribera d'Alcalà M, Falciatore A. 2017. Light sensing and responses in marine microalgae. Current Opinion in Plant Biology 37, 70-77.

Keller MD, Selvin RC, Claus W, Guillard RRL. 1987. Media for the culture of oceanic ultraphytoplankton. Journal of Phycology 23, 633-638.

Kianianmomeni A, Hallmann A. 2014. Algal photoreceptors: in vivo functions and potential applications. Planta 239, 1-26.

Kim D, Pertea G, Trapnell C, Pimentel H, Kelley R, Salzberg SL. 2013. TopHat2: accurate alignment of transcriptomes in the presence of insertions, deletions and gene fusions. Genome Biology doi: 10.1186/gb-2013-14-4-r36

Kirkham AR, Lepère C, Jardillier LE, Not F, Bouman H, Mead A, Scanlan DJ. 2013. A global perspective on marine photosynthetic picoeukaryote community structure. The ISME Journal: Multidisciplinary Journal of Microbial Ecology 7, 922-936.

Klughammer C, Schreiber U. 2008. Complementary PS II quantum yields calculated from simple fluorescence parameters measured by PAM fluorometry and the Saturation Pulse method. PAM Application Notes 1, 27-35.

Kolde R. 2019. pheatmap: Pretty Heatmaps. https://CRAN.R-project.org/package=pheatmap

Korbee N, Figueroa FL, Aguilera J. 2005. Effect of light quality on the accumulation of photosynthetic pigments, proteins and mycosporine-like amino acids in the red alga *Porphyra leucosticta* (Bangiales, Rhodophyta). Journal of Photochemistry and Photobiology B: Biology 80, 71-78.

Kramer D, Johnson G, Kiirats O, Edwards G. 2004. New fluorescence parameters for the determination of Q A redox state and excitation energy fluxes. Photosynthesis Research 79, 209-218.

Kulk G, Platt T, Dingle J, *et al*. . 2020. Primary production, an index of climate change in the ocean: satellite-based estimates over two decades. Remote Sensing doi: 10.3390/rs12050826

Kume A, Akitsu T, Nasahara KN. 2018. Why is chlorophyll *b* only used in light-harvesting systems? Journal of Plant Research 131, 961-972.

Langmead B, Salzberg SL. 2012. Fast gapped-read alignment with Bowtie 2. Nature Methods 9, 357-359.

Lehmuskero A, Skogen Chauton M, Boström T. 2018. Light and photosynthetic microalgae: A review of cellular- and molecular-scale optical processes. Progress in Oceanography 168, 43-56.

Li Y, Cai X, Gu W, Wang G. 2020. Transcriptome analysis of carotenoid biosynthesis in *Dunaliella salina* under red and blue light. Journal of Oceanology and Limnology 38, 177-185.

Lichtenthaler HK. 1987. Chlorophylls and carotenoids: Pigments of photosynthetic biomembranes. Methods in Enzymology, Vol. 148: Academic Press, 350-382.

Lim G, Chang Y, Huh W-K. 2020. Phosphoregulation of Rad51/Rad52 by CDK1 functions as a molecular switch for cell cycle–specific activation of homologous recombination. Science Advances doi: 10.1126/sciadv.aay2669

Limardo AJ, Sudek S, Choi CJ, Poirier C, Rii YM, Blum M, Roth R, Goodenough U, Church MJ, Worden AZ. 2017. Quantitative biogeography of picoprasinophytes establishes ecotype distributions and significant contributions to marine phytoplankton. Environmental Microbiology 19, 3219-3234.

Liu J, van Iersel MW. 2021. Photosynthetic physiology of blue, green, and red Light: Light Intensity Effects and Underlying Mechanisms. Frontiers in Plant Science doi: 10.3389/fpls.2021.619987

Liu X-y, Hong Y, Gu W-p. 2021. Influence of light quality on *Chlorella* growth, photosynthetic pigments and high-valued products accumulation in coastal saline-alkali leachate. Water Reuse 11, 301-311.

Luck M, Velázquez Escobar F, Glass K, Sabotke M-I, Hagedorn R, Corellou F, Siebert F, Hildebrandt P, Hegemann P. 2019. Photoreactions of the Histidine Kinase Rhodopsin Ot-HKR from the marine picoalga *Ostreococcus tauri*. Biochemistry 58, 1878-1891.

Maere S, Heymans K, Kuiper M. 2005. BiNGO: a Cytoscape plugin to assess overrepresentation of gene ontology categories in biological networks. Bioinformatics doi: 10.1093/bioinformatics/bti551

Maltsev Y, Maltseva K, Kulikovskiy M, Maltseva S. 2021. Influence of light conditions on microalgae growth and content of lipids, carotenoids, and fatty acid composition. Biology doi: 10.3390/biology10101060

Mullaney PF, Van Dilla MA, Coulter JR, Dean PN. 1969. Cell sizing: a light scattering photometer for rapid volume determination. Review of Scientific Instruments 40, 1029-1032.

Mullin MM. 2001. Plankton. In: Cochran JK, Bokuniewicz HJ, Yager PL, eds. *Encyclopedia of Ocean Sciences (Third Edition)*. Oxford: Academic Press, 613-614.

Munné-Bosch S, Cela J. 2006. Effects of water deficit on photosystem II photochemistry and photoprotection during acclimation of lyreleaf sage (*Salvia lyrata L.*) plants to high light. Journal of Photochemistry and Photobiology B-Biology 85, 191-197.

Neun S, Hintz NH, Schröder M, Striebel M. 2022. Phytoplankton response to different light colors and fluctuation frequencies. Frontiers in Marine Science doi: 10.3389/fmars.2022.824624

Palenik B, Grimwood J, Aerts A, *et al*. . 2007. The tiny eukaryote *Ostreococcus* provides genomic insights into the paradox of plankton speciation. Proceedings of the National Academy of Sciences of the United States of America 104, 7705-7710.

Patelou M, Infante C, Dardelle F, Randewig D, Kouri ED, Udvardi MK, Tsiplakou E, Mantecón L, Flemetakis E. 2020. Transcriptomic and metabolomic adaptation of *Nannochloropsis gaditana* grown under different light regimes. Algal Research 45, 101735.

Perdomo JA, Capó-Bauçà S, Carmo-Silva E, Galmés J. 2017. Rubisco and Rubisco Activase play an important role in the biochemical limitations of photosynthesis in rice, wheat, and maize under high temperature and water deficit. Frontiers in Plant Science doi: 10.3389/fpls.2017.00490

Petroutsos D, Tokutsu R, Maruyama S *et al.* . 2016. A blue-light photoreceptor mediates the feedback regulation of photosynthesis. Nature 537, 563–566.

Platt T, Gallegos CL, Harrison WG. 1980. Photoinhibition of photosynthesis in natural assemblages of marine phytoplankton. Journal of Marine Research 38, 687-701.

Portis AR, Jr. 2003. Rubisco Activase - Rubisco's catalytic chaperone. Photosynthesis Research 75, 11-27.

Potes M, Costa MJ, Salgado R, Bortoli D, Serafim A, Moigne PL. 2013. Spectral measurements of underwater downwelling radiance of inland water bodies. Tellus A: Dynamic Meteorology and Oceanography doi: 10.3402/tellusa.v65i0.20774

Quinlan AR, Hall IM. 2010. BEDTools: a flexible suite of utilities for comparing genomic features. Bioinformatics doi: 10.1093/bioinformatics/btq033

Ralph PJ, Gademann R. 2005. Rapid light curves: A powerful tool to assess photosynthetic activity. Aquatic Botany 82, 222-237.

Raven JA. 1996. The bigger the fewer: size, taxonomic diversity and the range of chlorophyll(Ide) pigments in oxygen-evolving marine photolithotrophs. Journal of the Marine Biological Association of the United Kingdom 76, 211-217.

Redekop P, Sanz-Luque E, Yuan Y, Villain G, Petroutsos D, Grossman AR. 2022. Transcriptional regulation of photoprotection in dark-to-light transition - More than just a matter of excess light energy. Science Advances doi: 10.1126/sciadv.abn1832

Rii YM, Duhamel S, Bidigare RR, Karl DM, Repeta DJ, Church MJ. 2016. Diversity and productivity of photosynthetic picoeukaryotes in biogeochemically distinct regions of the South East Pacific Ocean. Limnology and Oceanography 61, 806-824.

Rochet M, Legendre L, Demers S. 1986. Photosynthetic and pigment responses of sea-ice microalgae to changes in light intensity and quality. Journal of Experimental Marine Biology and Ecology 101, 211-226.

Rodriguez F, Derelle E, Guillou L, Le Gall F, Vaulot D, Moreau H. 2005. Ecotype diversity in the marine picoeukaryote *Ostreococcus* (Chlorophyta, Prasinophyceae). Environmental Microbiology 7, 853-859.

Sanfilippo JE, Garczarek L, Partensky F, Kehoe DM. 2019. Chromatic Acclimation in Cyanobacteria: A Diverse and Widespread Process for Optimizing Photosynthesis. Annual Review of Microbiology 73, 407-433.

Schaum CE, Rost B, Collins S. 2016. Environmental stability affects phenotypic evolution in a globally distributed marine picoplankton. The ISME Journal: Multidisciplinary Journal of Microbial Ecology 10, 75-84.

Schellenberger Costa B, Jungandreas A, Jakob T, Weisheit W, Mittag M, Wilhelm C. 2012. Blue light is essential for high light acclimation and photoprotection in the diatom Phaeodactylum tricornutum. Journal of Experimental Botany 64, 483-493.

Schubert H, Sagert S, Forster R. 2001. Evaluation of the different levels of variability in the underwater light field of a shallow estuary. Helgoland Marine Research 55, 12-22.

Sinha N, Eirich J, Finkemeier I, Grimm B. 2022. Glutamate 1-semialdehyde aminotransferase is connected to GluTR by GluTR-binding protein and contributes to the rate-limiting step of 5-aminolevulinic acid synthesis. Plant Cell 34, 4623-4640.

Six C, Finkel Z, Rodriguez F, Marie D, Partensky F, Campbell D. 2008. Contrasting photoacclimation costs in ecotypes of the marine eukaryotic picoplankter *Ostreococcus*. Limnology and Oceanography 53, 255-265.

Six C, Sherrard R, Lionard M, Roy S, Campbell D. 2009. Photosystem II and pigment dynamics among ecotypes of the green alga *Ostreococcus*. Plant Physiology 151, 379-390.

Subirana L, Péquin B, Michely S, et al. . 2013. Morphology, Genome Plasticity, and Phylogeny in the Genus *Ostreococcus* Reveal a Cryptic Species, *O. mediterraneus* sp. nov. (Mamiellales, Mamiellophyceae). Protist 164, 643-659.

Sullivan S, Petersen J, Blackwood L, Papanatsiou M, Christie JM. 2016. Functional characterization of *Ostreococcus tauri* phototropin. New Phytologist 209, 612-623.

Sun D, Li Y, Wang Q, Lv H, Le C, Huang C, Gong S. 2010. Partitioning particulate scattering and absorption into contributions of phytoplankton and non-algal particles in winter in Lake Taihu (China). Hydrobiologia 644, 337-349.

The_Galaxy_Community. 2022. The Galaxy platform for accessible, reproducible and collaborative biomedical analyses: 2022 update. Nucleic Acids Research 50, W345-W351.

Tilzer M, Stambler N, Lovengreen C. 1995. The role of phytoplankton in determining the underwater light climate in Lake Constance. Hydrobiologia 316, 161-172.

Trapnell C, Hendrickson DG, Sauvageau M, Goff L, Rinn JL, Pachter L. 2013. Differential analysis of gene regulation at transcript resolution with RNA-seq. Nature Biotechnology 31, 46-53.

Valle KC, Nymark M, Aamot I, Hancke K, Winge P, Andresen K, Johnsen G, Brembu T, Bones AM. 2014. System Responses to Equal Doses of Photosynthetically Usable Radiation of Blue, Green, and Red Light in the Marine Diatom Phaeodactylum tricornutum. PLoS ONE doi: 10.1371/journal.pone.0114211

Van Heukelem L, Thomas CS. 2001. Computer-assisted high-performance liquid chromatography method development with applications to the isolation and analysis of phytoplankton pigments. The Journal of Chromatography A 910, 31-49.

Wallen DG, Geen GH. 1971. Light quality in relation to growth, photosynthetic rates and carbon metabolism in two species of marine plankton algae. Marine Biology 10, 34-43.

Wang Y, Folta KM. 2013. Contributions of green light to plant growth and development. American Journal of Botany 100, 70-78.

Wei L, You W, Gong Y, El Hajjami M, Liang W, Xu J, Poetsch A. 2020. Transcriptomic and proteomic choreography in response to light quality variation reveals key adaption mechanisms in marine *Nannochloropsis oceanica*. Science of The Total Environment doi: 10.1016/j.scitotenv.2020.137667

Weirauch MT, Yang A, Albu M, *et al*. . 2014. Determination and inference of eukaryotic transcription factor sequence specificity. Cell 158, 1431-1443.

Worden A, Nolan J, Palenik B. 2004. Assessing the dynamics and ecology of marine picophytoplankton: The importance of the eukaryotic component. Limnology and Oceanography 49, 168-179.

Xu L, Pan W, Yang G, Tang X, Martin RM, Liu G, Zhong C. 2021. Impact of light quality on freshwater phytoplankton community in outdoor mesocosms. Environmental Science and Pollution Research 28, 58536-58548.

Yuan H, Zhang X, Jiang Z, Wang X, Wang Y, Cao L, Zhang X. 2020. Effect of light spectra on microalgal biofilm: Cell growth, photosynthetic property, and main organic composition. Renewable Energy 157, 83-89.

Table 1: Identification of red, blue and green light-specific genes by RNA-Seq. Differentially expressed genes were first identified in pairwise comparisons between light conditions. Specific light quality responses were then identified as genes that were either upregulated or downregulated under one wavelength relative to both others.

Differential expression	Number of DEGs	Light quality response	Number of light quality-responsive genes
Blue > Red	706	Up-Blue (Blue > Red AND Green)	536
Blue > Green	807		
Blue < Red	661	Down-Blue (Blue < Red AND Green)	472
Blue < Green	746		
Red > Blue	666	Up-Red (Red > Blue AND Green)	32
Red > Green	237		
Red < Blue	706	Down-Red (Red < Blue AND Green)	14
Red < Green	113		
Green > Blue	746	Up-Green (Green > Blue AND Red)	32
Green > Red	113		
Green < Blue	807	Down-Green (Green < Blue AND Red)	159
Green < Red	237		

Table 2. Putative regulatory motifs in the promoters of light quality-responsive genes. These were identified as over-represented sequences in the 5' upstream region of light quality-responsive genes relative to the whole genome. Cognate transcription factors were identified based on the closest match to a predicted transcription factor binding motif within the Cis-BP database 2.0 (Weirauch *et al.*, 2014).

Gene cluster	Motif	Frequency within cluster	Frequency genome-wide	p value	Closest predicted transcription factor binding motif
Up-red		9 / 32 (30%)	213 / 7923 (2.6%)	$1.4\ 10^{-7}$	 MYB Od06g01160
Up-blue	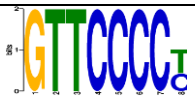	33/536 (6.1%)	117/7923 (1.4%)	$1.7\ 10^{-10}$	 E2F Od10g00570
		163/536 (30%)	1632 / 7923 (20%)	$1.6\ 10^{-7}$	 MYB Od12g02060
Down-red		7 / 14 (50%)	100 / 7923 (1.2 %)	$2.1\ 10^{-10}$	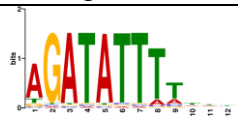 MYB (CCA1) Od04g00700
Down-blue		91 / 472 (19%)	404 / 7923 (5.0%)	$2.1\ 10^{-25}$	 MYB Od06g01160
		24/472 (5.0 %)	25/7923 (0.3%)	$3.5\ 10^{-12}$	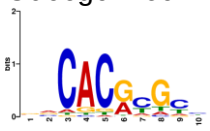 bHLH Od20g02280

Table 3: Overrepresented functional categories in RCC809 light quality-responsive genes

GO: Biological Process	Corrected p-value	Number of genes (frequency)	Number genome-wide (frequency)
Downregulated in green light			
DNA replication	$5.7\ 10^{-10}$	18 (18%)	89 (2%)
DNA duplex unwinding	$1.1\ 10^{-02}$	5 (4.9%)	24 (0.5%)
Nitrate transport	$1.8\ 10^{-02}$	2 (0.2%)	2 (0.04%)
Upregulated in red light			
NADPH regeneration	$2.6\ 10^{-03}$	4 (16%)	29 (0.7%)
Glycolysis	$1.3\ 10^{-02}$	3 (12%)	33 (0.8%)
Gluconeogenesis	1.4510^{-02}	3 (12%)	37 (0.9%)
Upregulated in blue light			
Cellular response to stress	$7.3\ 10^{-03}$	29 (11%)	204 (4.8%)
DNA-dependent DNA replication	$7.8\ 10^{-03}$	11 (4.1%)	42 (1.0%)
Chromosome segregation	$1.9\ 10^{-02}$	7 (2.7%)	21 (0.5%)
Tricarboxylic acid cycle	$2.2\ 10^{-02}$	9 (3.4%)	37 (0.9%)
Downregulated in blue light			
Pigment biosynthetic process	$1.6\ 10^{-07}$	18 (6.6%)	47 (1.1%)
Chl biosynthetic process	$9.3\ 10^{-07}$	11 (5.1%)	19 (0.4%)
Glycolysis	$3.9\ 10^{-03}$	9 (3.3%)	33 (0.8%)
Gluconeogenesis	$7.9\ 10^{-03}$	9 (3.3%)	37 (0.9%)
Carotenoid (tetraterpenoid) biosynthetic process	$1.0\ 10^{-02}$	5 (1.8%)	12 (0.3%)
Nicotinamide nucleotide metabolic process	$1.5\ 10^{-02}$	9 (3.2%)	41 (1.0%)
Lipid biosynthetic process	$1.6\ 10^{-02}$	18 (6.5%)	126 (3.0%)
Photosynthesis	$2.4\ 10^{-02}$	15 (5.5%)	101 (2.4%)
Glucan biosynthetic process	$4.7\ 10^{-02}$	4 (1.5%)	11 (0.3%)
Reductive pentose-phosphate cycle	$4.7\ 10^{-02}$	2(0.7%)	2 (0.05%)
Endosome organization	$4.7\ 10^{-02}$	2(0.7%)	2 (0.05%)
Phylloquinone biosynthetic process	$4.7\ 10^{-02}$	2(0.7%)	2 (0.05%)

Figure legends

Fig. 1 Effects of light quality on RCC809 cultures. (A) Growth kinetics. (B) Cell sizes estimated by FSC-H relative to singlet beads. Cultures were grown under red, blue or green monochromatic light at 4 μmol m^{-2} s^{-1}. Data are means and standard errors from three replicate experiments. Different letters indicate significant differences ($p<0.05$) between light conditions and ns indicates no significant differences, as determined by Student's t-tests.

Fig. 2 Transcriptomic analysis of RCC809 responses to light quality. (A) Experimental design. Cells were grown to mid-log phase then transferred to red, green or blue monochromatic light at 4 μmol m^{-2} s^{-1} for 72 h. Cultures were then sampled for RNA-Seq analyses. Light quality-responsive genes were initially identified through pairwise comparison of expression levels between light qualities. Responses specific to individual light qualities were then identified as differences in gene expression that were observed between one light quality and both others. (B) Principal component analysis of gene expression data. Red, green and blue arrows represent the variable vectors for individual samples under the corresponding light conditions. (C) Heatmap of differentially expressed genes (DEGs) identified from the RNA-Seq analysis. Columns correspond to individual samples. Rows correspond to individual genes, clustered by Jensen-Shannon distance. Color from red to blue indicates log fold changes relative to mean expression levels. (D) Number of genes showing upregulation (Up) or downregulation (Down) specific to red, green or blue light.

Fig. 3 Analysis of pigment contents in RCC809 following acclimation to different light qualities. (A) Carotenoid pigments. (B) Total xanthophylls relative to chlorophyll *a* (chl*a*). Z, A and V correspond to zeaxanthin, antheraxanthin and violaxanthin, respectively. (C) Xanthophyll depoxidation state (DPS), calculated as (Z + 0.5A) / (V + A + Z). (D) Chls and chl derivatives. Levels are expressed relative to chl*a*. (E) Chl*a* to Chl*b* ratio. Red, green and blue bars correspond to samples acclimated to red, green and blue monochromatic light for 72 h. Data are means and standard errors from triplicate experiments. Different letters indicate significant differences ($p<0.05$) between light conditions and ns indicates no significant differences, as determined by Student's t-tests.

Fig. 4 Effect of light quality on photosynthetic parameters in RCC809. (A-D) Rapid light curves showing (A) the quantum yield of Photosystem II (ΦPSII), (B) the relative electron transport rate (rETR), (C) the quantum yield of unregulated non-photochemical energy loss

in PSII (ΦNO), and (D) the quantum yield of regulated non-photochemical energy loss in PSII (ΦNPQ) as a function of irradiance (photosynthetically active radiation or PAR) for cultures acclimated to either red, green or red light. ΦPSII + ΦNPQ, + ΦNO =1 (E) Derived photosynthetic parameters, including the maximum quantum yield, maximum rETR, initial slope of the rETR curve (Alpha), and irradiance at the onset of light saturation (IK). Data are the mean and standard error from triplicate experiments. Different letters indicate significantly different values ($p<0.05$) as determined using Student's t-tests.

Fig. 5 Light quality responses in the lagoon species OTTH0595, also known as *O. tauri*. (A) Growth kinetics. (B) and (C) Levels of chlorophylls and chlorophyll derivatives relative to chl*a*, and levels of carotenoid pigments relative to total carotenoids. Red, green and blue bars correspond to samples acclimated to red, green and blue monochromatic light for 72 h. Data are the mean and standard error from triplicate experiments. Different letters indicate significant differences ($p < 0.05$) between light conditions and ns indicates no significant differences, as determined by Student's t-tests. (D) and (E) Photosynthetic light-response curves showing the quantum yield of Photosystem II (ΦPSII) and relative electron transport rate (rETR) as a function of irradiance (photosynthetically active radiation or PAR), for cultures acclimated to either red, green or red light. Data are the mean and standard error from triplicate experiments. (F) Frequency of motif conservation between RCC809 red and blue light-responsive genes and their OTTH0595 homologues. Solid red and blue bars correspond to genes upregulated under red and blue light, respectively. Hatched red and blue bars correspond to genes downregulated under red and blue light.

Fig. 6. Conceptual model showing how the RCC809 ecotype of *Ostreococcus* may alter its physiology in response to changes in light quality as it is moved up and down the water column. The colour of text boxes indicates the specific wavelengths inducing the responses. Coloured wedges on the left represent the decrease in red, green and blue light wavelengths with increasing depth. Perception of red may signal proximity to the surface. This may enable cells to anticipate exposure to high light intensities by increasing their potential for photoprotection as well as their ability to utilise light energy. Further, increased production of blue light-absorbing pigments may maximise light capture in the lower part of the euphotic zone where only blue wavelengths can penetrate. Green and red clouds on the right represent increased proportions of green and red wavelengths, caused by the presence of phytoplankton, dissolved organic matter and other sediments in shallow coastal waters. Detection of these wavelengths may be interpreted as unfavourable conditions for growth and lead to slower cell division.

Figure 1

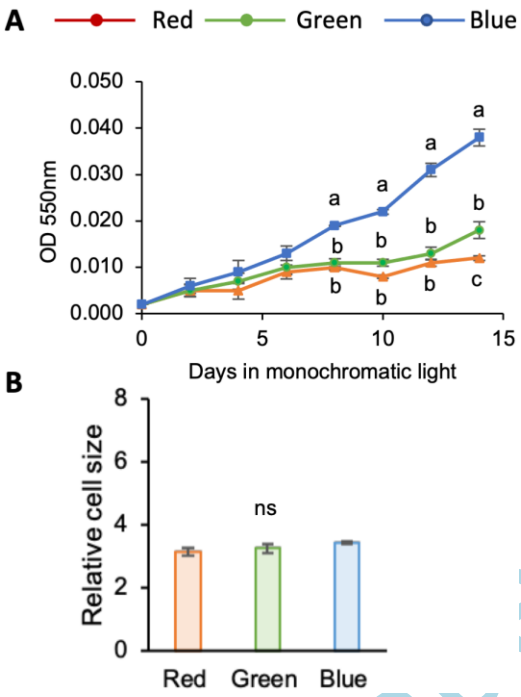

Figure 2

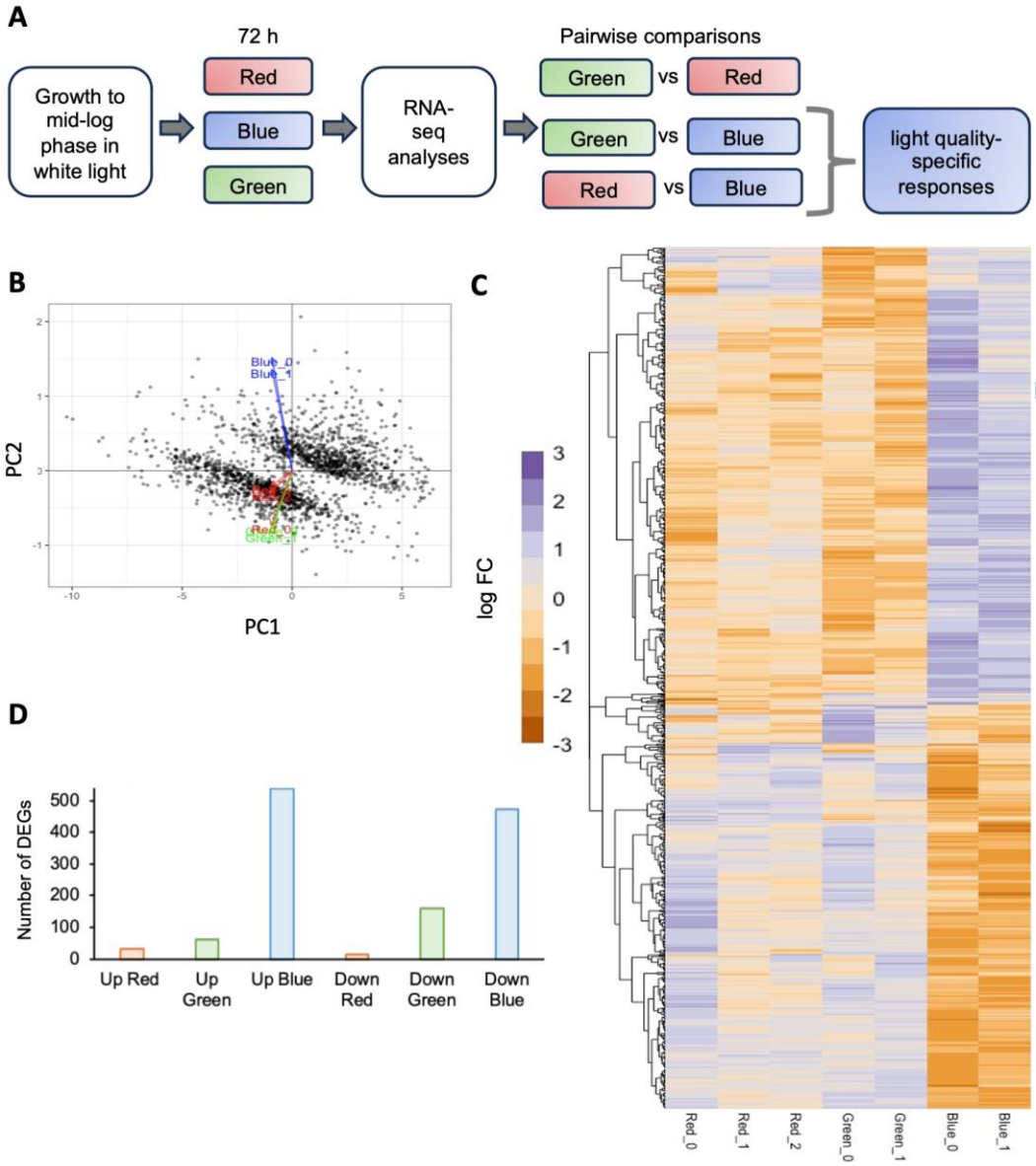

Figure 3

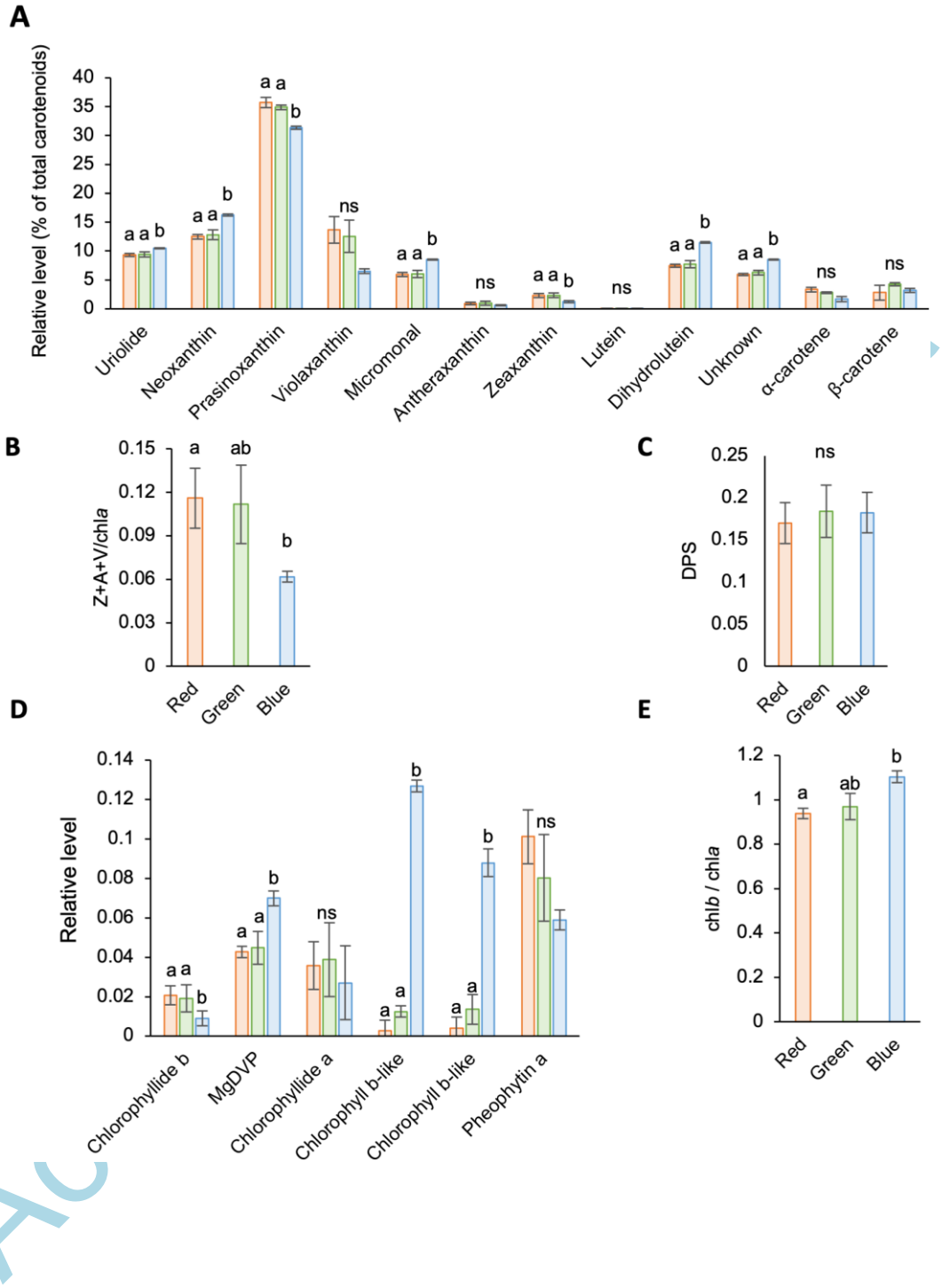

Figure 4

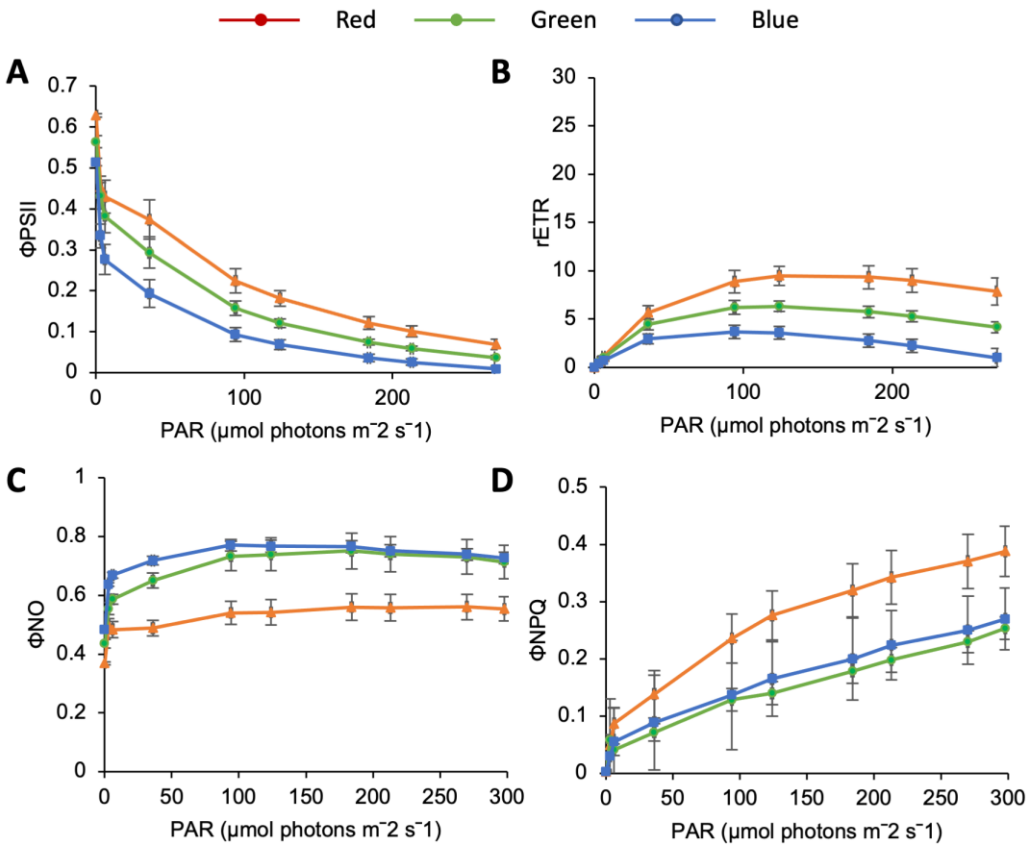

E

Light quality	Maximum quantum yield of PSII (ΦPSII)	Maximum rETR	Alpha	IK
Red	0.63 ±0.00 (a)	9.48 ±0.00 (a)	0.194 ±0.030 (a)	50.4 ±8.3 (a)
Green	0.57 ±0.00 (b)	6.31 ±0.01 (b)	0.148 ±0.007 (ab)	43.6 ±3.1 (b)
Blue	0.52 ±0.00 (b)	3.67 ±0.01 (c)	0.123 ±0.017 (b)	31.6 ±2.4 (c)

Figure 5

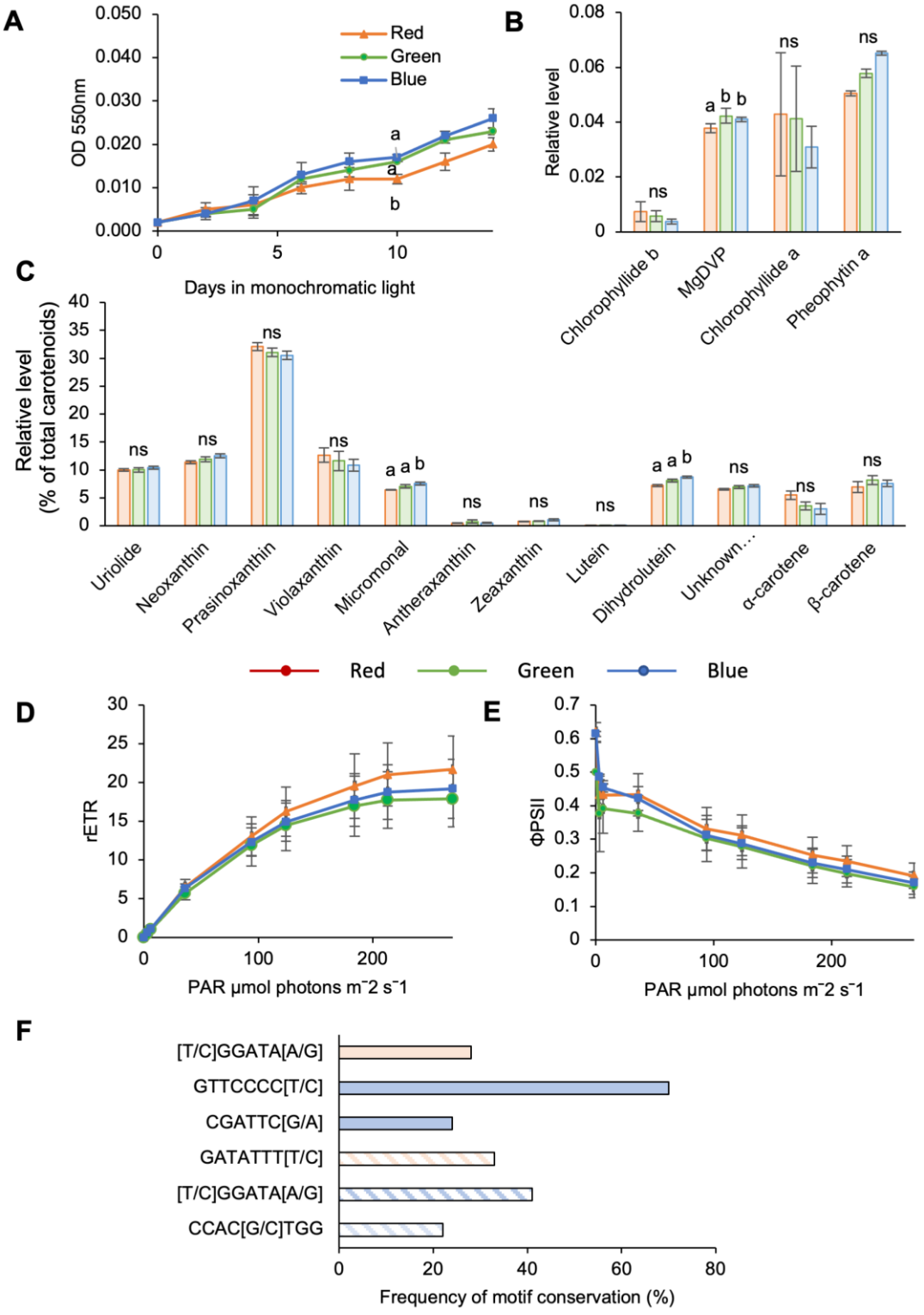

Figure 6